

*Total oxidation of propane and naphthalene from emission sources with supported cobalt catalysts*

**María Silvia Leguizamón Aparicio & Ileana Daniela Lick**

**Reaction Kinetics, Mechanisms and Catalysis**

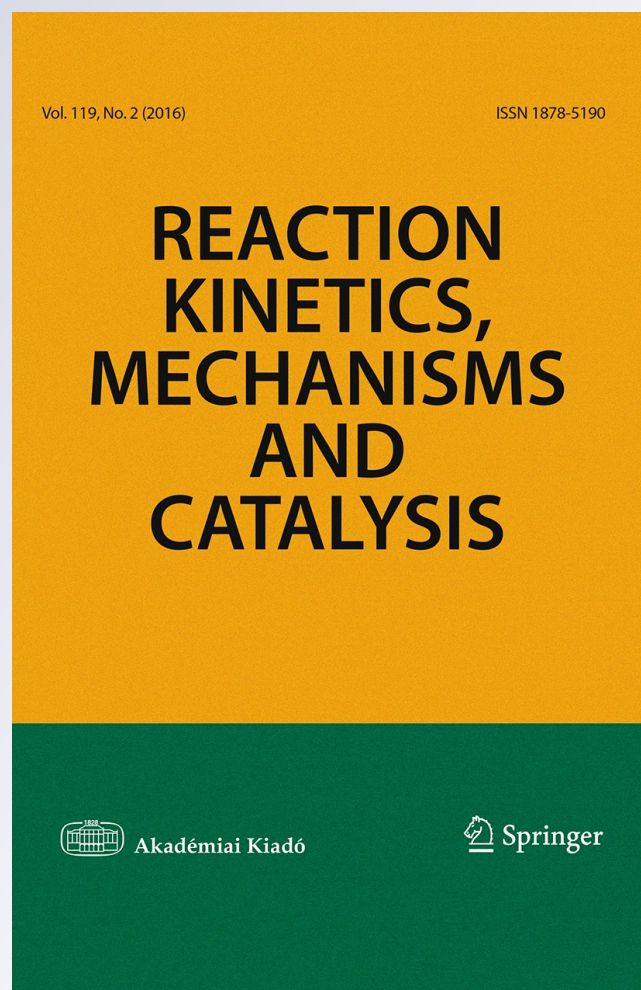
ISSN 1878-5190

Volume 119

Number 2

Reac Kinet Mech Cat (2016) 119:469-479

DOI 10.1007/s11144-016-1052-3



**Your article is protected by copyright and all rights are held exclusively by Akadémiai Kiadó, Budapest, Hungary. This e-offprint is for personal use only and shall not be self-archived in electronic repositories. If you wish to self-archive your article, please use the accepted manuscript version for posting on your own website. You may further deposit the accepted manuscript version in any repository, provided it is only made publicly available 12 months after official publication or later and provided acknowledgement is given to the original source of publication and a link is inserted to the published article on Springer's website. The link must be accompanied by the following text: "The final publication is available at [link.springer.com](http://link.springer.com)".**



# Total oxidation of propane and naphthalene from emission sources with supported cobalt catalysts

María Silvia Leguizamón Aparicio<sup>1</sup> ·  
Ileana Daniela Lick<sup>1</sup>

Received: 12 April 2016 / Accepted: 7 July 2016 / Published online: 15 July 2016  
© Akadémiai Kiadó, Budapest, Hungary 2016

**Abstract** Propane and naphthalene combustion reactions were studied in the presence of  $\text{CoO}_x/\text{SiO}_2$  catalysts. The catalysts were prepared by impregnation with four different levels of concentration (1, 5, 10 and 15 wt%) and characterized by several physicochemical techniques such as BET, DRX, SEM–EDS, TPR and UV–Vis DRS. TPR and UV–Vis DRS results reveal the presence of  $\text{Co}_3\text{O}_4$ -type species in all the studied catalysts, which are the active species for the combustion of both hydrocarbons.  $\text{CoO}_x(5)/\text{SiO}_2$ , which was the most active catalyst for the combustion of propane, presented also Co(II) ions in an octahedral environment, and this phase was the one responsible for the increase of the activity. For naphthalene combustion, the catalytic activity depends on the metal loading, the catalysts with higher loading being more active.

**Keywords** Combustion · Hydrocarbons · Propane · Naphthalene

## Introduction

The control of air polluting processes has tightened in the last decades. High concentrations of volatile organic compounds (VOCs) are released to the atmosphere by industries and motor vehicles, causing serious environmental

---

**Electronic supplementary material** The online version of this article (doi:[10.1007/s11144-016-1052-3](https://doi.org/10.1007/s11144-016-1052-3)) contains supplementary material, which is available to authorized users.

---

✉ Ileana Daniela Lick  
ilick@quimica.unlp.edu.ar

<sup>1</sup> Departamento de Química, Facultad de Ciencias Exactas, CINDECA (CCT-La Plata-CONICET-UNLP), Calle 47 No 257, La Plata, 1900 Buenos Aires, Argentina

damage. Catalytic oxidation is one of the most widely used methods to remove VOCs, converting them into carbon dioxide and water [1].

Alkanes in gaseous emissions contain between 2 and 10 carbons. Propane is one of the most difficult short-chain alkanes to destroy [2, 3] and may be released to the atmosphere from motor vehicle emissions, especially when LPG (a mixture of light hydrocarbons composed primarily of butane and propane) is used as fuel.

In addition, emissions contain polycyclic aromatic hydrocarbons (PAHs), which are carcinogenic and mutagenic to human beings exposed to this type of pollution. Naphthalene is the most volatile of the PAHs and is a component of diesel and jet fuel.

It is well known that noble metals such as Pd and Pt [4–8] are very active in the catalytic combustion of hydrocarbons. A more economical alternative is the use of transition metal oxides [9, 10]. Several formulations of these catalysts decrease the hydrocarbon combustion temperature. Among them, cobalt oxide and manganese oxide seem to show greater catalytic activity [11].

The catalytic combustion of propane has been widely studied. Instead, the catalytic combustion of PAHs, such as naphthalene, has been scarcely reported in the literature [12, 13]. A review has been published by Ntainjua and Taylor, showing that most of the studies on the total oxidation of polycyclic aromatic hydrocarbons are concentrated in the last years. [14]. Because many of the catalytic systems proposed for removing VOCs have been previously studied for the combustion of linear hydrocarbons (HC), it was interesting to analyze their potential in the oxidation of PAHs. It should be noted that the performance of the catalysts suitable for HC cannot be similar to that of PAHs, as their C–C bonds are different [15].

When the active phase is an oxide, the support plays a key role, as has been recently reported by Aboukais et al. [11]. These authors investigated the catalytic combustion of toluene and PAHs using manganese oxide supported on  $\text{TiO}_2$ ,  $\text{Al}_2\text{O}_3$  and  $\text{SiO}_2$ .

Silica-supported cobalt catalysts are used in this study; the choice of this simple system is based on the properties of silica. This support provides a large surface area and high number of surface silanol groups which allows obtaining high dispersion of the supported phases. These catalysts are used in the catalytic combustion reaction of propane and naphthalene.

The activity of these catalysts in the presence of  $\text{NO}_x$  was analyzed as well, as this reactant is present in the emissions, and its influence on the activity of catalysts for VOCs removal has been scarcely reported.

## Experimental

### Catalyst preparation and characterization

The catalysts were prepared by impregnation of the support ( $\text{SiO}_2$ , Degussa 200) with  $\text{Co}(\text{NO}_3)_2 \cdot 6\text{H}_2\text{O}$  solution in an ammoniacal medium at room temperature (6 h). These experimental conditions were selected taking into account that they promote

the formation of complexes between cobalt ion and ammonia molecules. The amount of ammonia added is the one required to obtain a constant  $\text{NO}_3^-/\text{NH}_3$  molar ratio of ca. 0.1. The pH of the solution was kept around 10. After the impregnation step, the solution was filtered, and the precipitate was washed with distilled water and dried at  $100^\circ\text{C}$  for 18 h. Then, the solid was thermally treated in air.

The addition of ammonia solution to the cobalt solution changes the original color. This is attributed to a change in the ligands complexing the cobalt ion, which is initially water  $[\text{Co}(\text{H}_2\text{O})_6]^{2+}$  (pink). Water molecules are replaced by  $\text{NH}_3$ ; a change in the oxidation state of cobalt may also occur, resulting in the formation of an octahedral coordination compound between cobalt and ammonia,  $[\text{Co}(\text{NH}_3)_6]^{3+}$  (blue) or  $[\text{Co}(\text{NH}_3)_4(\text{OH})_2]^+$  (greenish-blue). Ammonia addition avoids the early formation of clusters. These compounds then hydrolyze and precipitate, giving  $\text{Co}(\text{OH})_n^{m+}$  species.

Silica-supported cobalt catalysts were prepared with several cobalt concentrations (1, 5, 10 and 15 wt%). The catalysts were obtained by calcination of the cobalt/silica precursors at  $600^\circ\text{C}$  for 2 h in air, after a heating ramp from 25 to  $600^\circ\text{C}$  at  $10^\circ\text{C}/\text{min}$ . The samples were designated  $\text{CoO}_x$  (y)/ $\text{SiO}_2$ , where y is the cobalt content (wt%).

### Catalyst characterization

The surface area of catalysts was determined by the BET method using Micromeritics Accusorb 2100E equipment.

X-ray diffraction (XRD) was performed on an X-ray diffractometer (Philips PW 1732/10) using  $\text{Cu K}_\alpha$  radiation and operated at 40 kV and 20 mA.

Energy dispersive X-ray spectroscopy (EDS) analyses were performed using a SEM Philips 505 microscope provided with an EDAX DX PRIME 10 energy dispersive X-ray analyzer.

TPR (temperature programmed reduction) experiments were carried out with conventional equipment. The TPR was performed using 10 % hydrogen in nitrogen (flow rate  $20\text{ cm}^3\text{ min}^{-1}$ ) with a heating rate of  $10^\circ\text{C}/\text{min}$  up to  $800^\circ\text{C}$ . The amount of sample loaded was 30 mg.

Diffuse reflectance spectroscopy (DRS) analyses were carried out in a Perkin Elmer Lambda 35 UV–VIS spectrometer.

### Catalytic activity

#### *Propane oxidation*

Catalysts were evaluated in an electrically heated fixed-bed quartz reactor containing 0.100 g of catalyst. The catalytic activity for propane oxidation was determined using a mixture of  $\text{NO}/\text{He}$ ,  $\text{C}_3\text{H}_8/\text{He}$ ,  $\text{O}_2/\text{He}$  and He to close the balance. The reaction flow contained 0 or 1000 ppm NO, 1000 ppm  $\text{C}_3\text{H}_8$  and 8 % v/v  $\text{O}_2$  (total flow rate =  $50\text{ mL min}^{-1}$ ). Reaction products were monitored with a TCD

Shimadzu GC (GC 2014). The separation of products was performed with an Alltech CTRI concentric column.

### *Naphthalene oxidation*

Catalysts were evaluated in an electrically heated fixed-bed quartz reactor containing 0.100 g of catalyst. The catalytic activity for naphthalene oxidation was determined using a mixture of 10 % O<sub>2</sub>, 90 % He and 150 ppm naphthalene. The total flow rate was 30 mL min<sup>-1</sup>.

The feed stream passes through a saturator where the naphthalene is placed. The saturator is kept at constant temperature by a thermostated bath at 25 °C to ensure constant vapor pressure. The rest of the flow system is kept at a higher temperature to avoid the undesired reverse sublimation of naphthalene.

Four analyses for each temperature were made and the average value is reported. Then, the reaction temperature is increased and, when the naphthalene vapor pressure stabilizes, the sampling procedure is performed.

## Results and discussion

### Catalyst characterization

BET surface areas and pore specific volume of the series of cobalt catalysts and the support are shown in Table 1. The results show that the pore volume decreases with the increment of the cobalt concentration, while that of the catalyst surface area increases, probably due to the formation of new supported particles that contribute to the total surface area.

XRD patterns of the catalysts were used to examine the supported crystalline species present. In the XRD pattern of the silica used, no well-defined diffraction lines appear in the range  $2\theta = 5^\circ\text{--}70^\circ$ , indicating the amorphous nature of the support. There is only a broad signal between  $2\theta = 18^\circ$  and  $30^\circ$ , which is associated with silica tetramers, SiO<sub>4</sub>.

The XRD patterns of CoO<sub>x</sub>(y)/SiO<sub>2</sub> catalysts are shown in Fig. 1. They do not exhibit diffraction lines characteristic of crystalline structures. Co<sub>3</sub>O<sub>4</sub>, a cobalt oxide species with a complete crystalline spinel structure, shows its main diffraction

**Table 1** BET surface area values and EDS results

Catalysts	Specific area (m <sup>2</sup> /g)	Pore volume (cm <sup>3</sup> /g)	Nominal ratio Co/Si	EDS Co/Si
SiO <sub>2</sub>	200	–	–	–
CoO <sub>x</sub> (1)/SiO <sub>2</sub>	162	1.22	0.010	0.044
CoO <sub>x</sub> (5)/SiO <sub>2</sub>	176	1.23	0.054	0.098
CoO <sub>x</sub> (10)/SiO <sub>2</sub>	196	1.18	0.113	0.149
CoO <sub>x</sub> (15)/SiO <sub>2</sub>	224	1.04	0.179	0.178

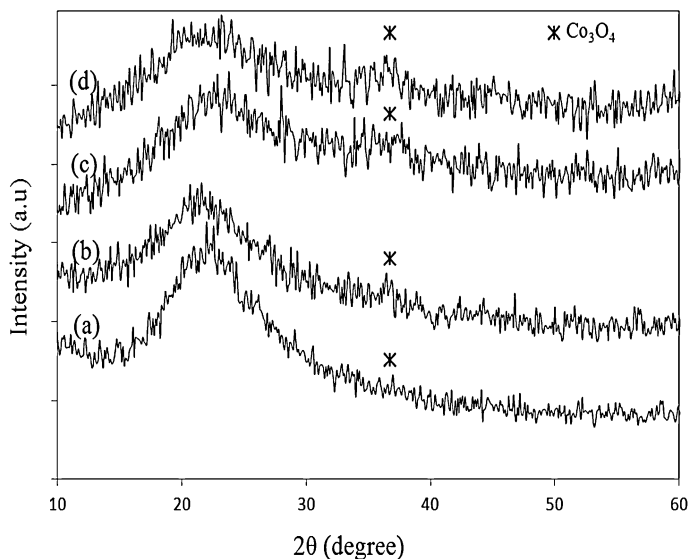


**Fig. 1** XRD patterns. *a*  $\text{CoO}_x(1)/\text{SiO}_2$ , *b*  $\text{CoO}_x(5)/\text{SiO}_2$ , *c*  $\text{CoO}_x(10)/\text{SiO}_2$ , *d*  $\text{CoO}_x(15)/\text{SiO}_2$

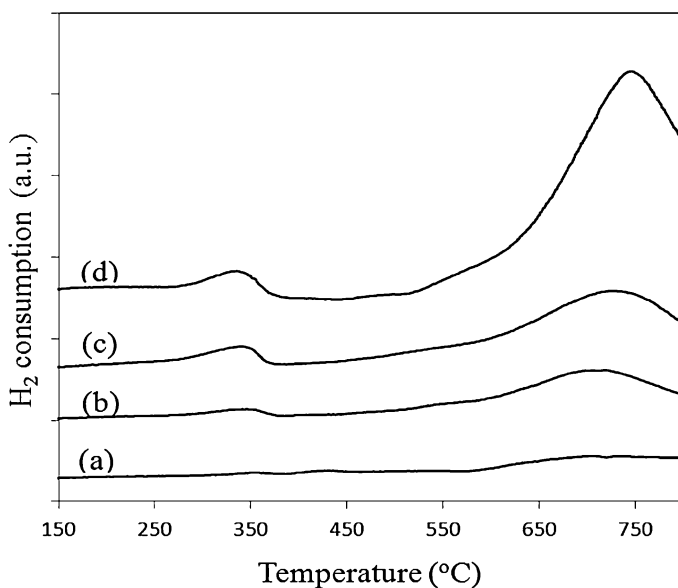


**Fig. 2** TPR patterns. *a*  $\text{CoO}_x(1)/\text{SiO}_2$ , *b*  $\text{CoO}_x(5)/\text{SiO}_2$ , *c*  $\text{CoO}_x(10)/\text{SiO}_2$ , *d*  $\text{CoO}_x(15)/\text{SiO}_2$

lines at  $2\theta = 36.8^\circ$ ,  $65.35^\circ$ ,  $31.2^\circ$  and  $59.35^\circ$ , which do not clearly appear in the XRD patterns of the catalysts.

Cobalt EDS mappings on the catalyst surface (supplementary files) showed that the metal is uniformly distributed in all the samples, given that the analyses



**Table 2** Results of TPR analysis

Catalysts	Low-interaction region: 250–450 °C	High-interaction region: 600–800 °C
CoO <sub>x</sub> (1)/SiO <sub>2</sub>	350	705
CoO <sub>x</sub> (5)/SiO <sub>2</sub>	345	715
CoO <sub>x</sub> (10)/SiO <sub>2</sub>	340	730
CoO <sub>x</sub> (15)/SiO <sub>2</sub>	335	745

performed on different surface area regions yielded similar results. At higher cobalt concentration in the samples, the density in the mapping increases.

Table 1 lists the cobalt to silicon atomic ratios obtained by the semiquantitative surface analysis by energy dispersive X-ray spectroscopy and the Co/Si nominal ratio.

For the CoO<sub>x</sub>(1)/SiO<sub>2</sub>, CoO<sub>x</sub>(5)/SiO<sub>2</sub> and CoO<sub>x</sub>(10)/SiO<sub>2</sub> catalysts, the surface ratios (EDS) are greater than the nominal ratios, which suggests that cobalt species are mostly present on the particle surface of the support. This cannot be seen in the CoO<sub>x</sub>(15)/SiO<sub>2</sub> catalyst. The high cobalt content may favor the reaction of this transition metal with the silica silanol groups, forming new Co-silica species that strongly interact during the calcination process at 600 °C. It is worth noting that the formation of a complete cobalt silicate type structure cannot be expected as the calcination temperature is not high enough. TPR experiments were conducted to determine the presence of reducible cobalt phases and their interaction with the support.

Silica-supported cobalt catalysts mostly contain segregated oxide phases. The Co<sub>3</sub>O<sub>4</sub> reduces in two stages between 300 and 400 °C [16]. A signal at about 650 °C may be attributed to the reduction of Co(II) ions interacting with the support. TPR patterns recorded for CoO<sub>x</sub>(y)/SiO<sub>2</sub> catalysts are shown in Fig. 2.

In the reduction profiles, the area under the curve increases as the cobalt concentration in the catalysts is higher. All the catalysts exhibit reduction signals attributed to the reduction of mixed cobalt oxide and signals associated with the reduction of Co(II) ions interacting with the support. The TPR pattern of the CoO<sub>x</sub>(1)/SiO<sub>2</sub> catalyst shows reduction signals of very low intensity in the low-interaction region, 250–450 °C, as well as in the high-interaction region, 600–800 °C. At higher metal loading, the intensity of reduction signals increases and a reduction signal shift occurs. The temperatures of the maximum reduction signals are summarized in Table 2.

With increasing cobalt content, the signals in the low-interaction region shift towards lower temperature, which may be assigned to the segregation of supported oxide phases. In the high-interaction region, however, with increasing cobalt content, the cobalt–support interaction increases and the signals shift towards higher temperature. These structures may be cobalt hydrosilicate species, which have also been proposed for the Ni/SiO<sub>2</sub> system, suggesting the formation of species such as Ni<sub>3</sub>(OH)<sub>3</sub>Si<sub>2</sub>O<sub>5</sub>(OH) or Ni<sub>3</sub>(OH)<sub>2</sub>(Si<sub>2</sub>O<sub>5</sub>)<sub>2</sub> that reduce at approximately 600 °C [17]. Probably, the formation of these high-interaction species also affects the textural properties, decreasing the pore volume.

In order to analyze the chemical environment of cobalt as regards its coordination, DRS UV–Vis tests were carried out. Cobalt oxide phases are present



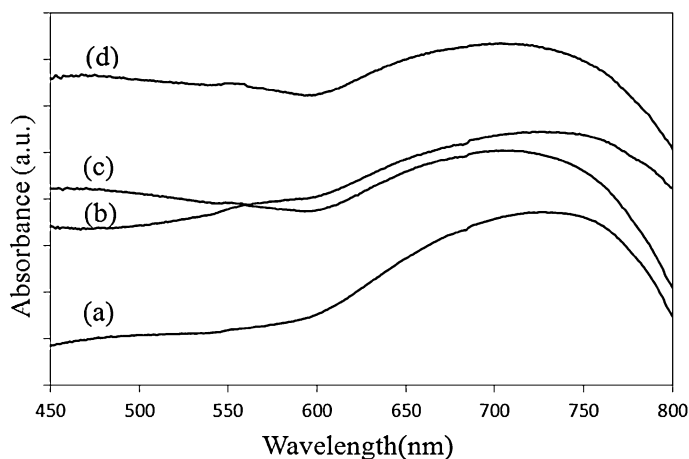


**Fig. 3** DRS spectra. *a* CoO<sub>x</sub>(1)/SiO<sub>2</sub>, *b* CoO<sub>x</sub>(5)/SiO<sub>2</sub>, *c* CoO<sub>x</sub>(10)/SiO<sub>2</sub>, *d* CoO<sub>x</sub>(15)/SiO<sub>2</sub>

on the catalysts with energy absorption bands between 800 and 700 nm, characteristic of Co<sub>3</sub>O<sub>4</sub> cobalt spinel due to the electronic transitions  $4A^2 \rightarrow ^2E$  and/or  $4T_{1g} \rightarrow ^2T_1, ^2T_2$ , which prevail in this type of spectrum (Fig. 3). These results agree with those reported by Girardon et al. [18].

In the spectra of catalysts with higher cobalt loading, this band shifts due to a slight change in coordination, towards shorter wavelengths. These results indicate that the bonds involved in electronic transitions are stronger. TPR yielded the same results with increasing reduction temperature of the species with a high metal–support interaction.

A small band appearing between 550 and 600 nm is attributed to the presence of Co(II) in octahedral positions due to the electronic transition  $4T_{1g}(F) \rightarrow 4T_{1g}(P)$ . Such a band indicates the presence of incomplete cobalt silicate type species, Co<sub>2</sub>SiO<sub>4</sub> [19]. The presence of CoO, where Co(II) is located in an octahedral environment, cannot be ruled out.

TPR and UV–Vis DRS results revealed the presence of Co<sub>3</sub>O<sub>4</sub> type species, but they have a smaller crystal size than that needed for XRD despite the high metal content in some samples. In similar catalysts prepared by other authors, the oxide species, Co<sub>3</sub>O<sub>4</sub>, were observed by XRD and TEM [20–22]. According to our results, the oxide and interaction species formed between cobalt and the support do not create large-size segregated crystal structures. Evidently, the prepared catalysts exhibit a high dispersion of the active phase.

## Catalytic activity

### *Catalytic combustion of propane*

In the absence of a catalyst, propane oxidizes at very high temperature when the oxidizing atmosphere is O<sub>2</sub>/He, reaching 50 % conversion at 600 °C. This

temperature, at which 50 % conversion is attained, is a widely used parameter in combustion reactions and is called T50. Silica calcined at 600 °C shows low catalytic activity and attains 50 % conversion at 560 °C. Fig. 4 and Table 3 show the catalytic results obtained with  $\text{CoO}_x(y)/\text{SiO}_2$  catalysts, such as conversion of propane ( $\text{C}_3\text{H}_8$ ) to carbon dioxide ( $\text{CO}_2$ ) versus temperature, using the  $\text{O}_2/\text{He}$  mixture as oxidizing agent.

Supported cobalt catalysts are active in the combustion of propane, and their activity depends on the metal loading. By taking T50 as catalytic activity indicator, the catalysts with a lower metal loading,  $\text{CoO}_x(1)/\text{SiO}_2$  and  $\text{CoO}_x(5)/\text{SiO}_2$ , are the most active. It is evident that an increase in cobalt content from 1 % w/w to 5 % w/w enhances the conversion. The T50 for  $\text{CoO}_x(1)/\text{SiO}_2$  is 370 °C and the T50 for  $\text{CoO}_x(5)/\text{SiO}_2$  is 275 °C. According to the characterization techniques, these two catalysts contain Co(II) species, where the coordination is tetrahedral, and also Co(III) ions in an octahedral environment, which are coordinations present in  $\text{Co}_3\text{O}_4$  cobalt spinel, as confirmed by TPR.

Besides, the DRS spectra of catalysts with a low metal loading show a band associated with the presence of Co(II) (d7) ions in an octahedral environment. When both Co(II) (d7), in high-spin tetrahedral coordination with 3 unpaired electrons, and Co(II) (d7), in octahedral coordination with one unpaired electron, oxidize to Co(III) (d6), they may move to a low-spin octahedral environment with all the electrons paired. This redox capacity may be a decisive factor in catalytic activity. Two suggested mechanisms have been accepted to explain naphthalene oxidation reaction: (i) The redox Mars-van Krevelen mechanism, where the metal oxide provides active oxygen for the reaction, and (ii) the Langmuir–Hinshelwood mechanism, which postulates the existence of active adsorption sites where the reactants interact and are turned into products, and that both mechanisms may contribute to catalytic activity [13]. Based on the results obtained, it is suggested there may be a first stage involving oxygen adsorption on metal oxide, where a

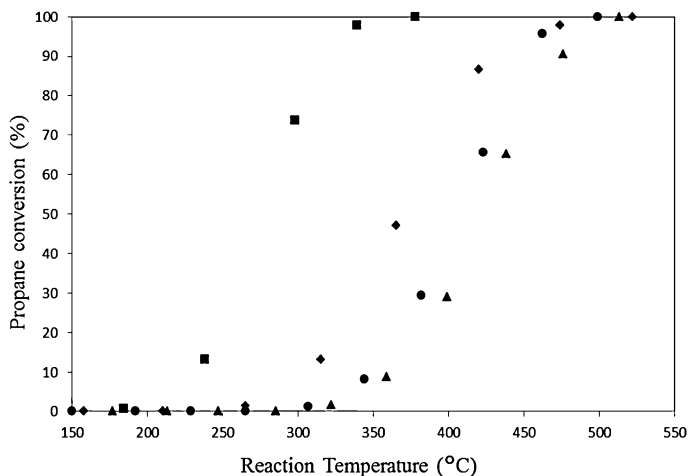


**Fig. 4** Catalytic activity in propane combustion. Filled diamond  $\text{CoO}_x(1)/\text{SiO}_2$ , filled square  $\text{CoO}_x(5)/\text{SiO}_2$ , filled triangle  $\text{CoO}_x(10)/\text{SiO}_2$ , filled circle  $\text{CoO}_x(15)/\text{SiO}_2$

**Table 3** T50 and T100 values obtained for the oxidation of propane and naphthalene

Catalyst	Propane				Naphthalene	
	T50 (°C)		T100 (°C)		T50 (°C)	T100 (°C)
	O <sub>2</sub> /He	NO/O <sub>2</sub> /He	O <sub>2</sub> /He	NO/O <sub>2</sub> /He		
CoO <sub>x</sub> (1)/SiO <sub>2</sub>	370	387	532	532	251	300
CoO <sub>x</sub> (5)/SiO <sub>2</sub>	275	287	347	347	235	300
CoO <sub>x</sub> (10)/SiO <sub>2</sub>	420	432	505	508	224	300
CoO <sub>x</sub> (15)/SiO <sub>2</sub>	408	420	480	513	228	270

charge transfer occurs and tetrahedral Co(II) may oxidize to octahedral Co(III), leading to the reduction of adsorbed O<sub>2</sub>. A redox reaction between this site and hydrocarbon is required so that the latter may be oxidized to CO<sub>2</sub>.

It may be assumed that in these catalysts a good dispersion of supported oxide phase has been achieved, and that these phases are responsible for the catalytic activity in propane combustion.

However, as the supported metal loading is increased, the conversion shifts to higher temperature. These catalysts, CoO<sub>x</sub>(10)/SiO<sub>2</sub> and CoO<sub>x</sub>(15)/SiO<sub>2</sub>, contain segregated oxide phases and cobalt species highly interacting with the support, which would not contribute to catalytic activity.

Due to the presence of nitric oxide (NO) in emission streams and in order to analyze the influence of this reagent on the catalytic activity, NO was added to the feed stream. In the absence of a catalyst, when the oxidizing atmosphere is O<sub>2</sub>/NO/He, the combustion of propane has a T50 of 550 °C. This T50 is lower than that obtained under an O<sub>2</sub>/He atmosphere.

Silica calcined at 600 °C has low catalytic activity in the presence of NO. Table 3 lists the temperature values at which T50 and T100 (temperature at which 100 % conversion is achieved) are obtained.

The presence of nitric oxide does not substantially change the catalytic activity, which is a very important fact because this contaminant is present in gaseous emissions. The temperatures increase by a few degrees, which may be attributed to a slight competitive adsorption of NO. This increase in temperature was also observed by Mrad et al. in the oxidation of propene using MgCu–Al(Fe) mixed oxides derived from hydroxalcalite-like compounds [23]. In this type of reaction, it is suggested that the hydrocarbon should adsorb on acid sites that, in this case, may be contributed by silica, and that oxygen and NO may adsorb on the sites contributed by cobalt. The catalyst with a metal loading of 5 % cobalt still is the most active of the series.

### Catalytic combustion of naphthalene

The catalytic activity in the combustion of naphthalene was measured. In the absence of a catalyst, the T50 for this reaction is 430 °C, and T100 is reached at 485 °C.

Table 3 and Fig. 5 show the catalytic results obtained with CoO<sub>x</sub>/SiO<sub>2</sub> catalysts, expressed as conversion of naphthalene (C<sub>8</sub>H<sub>10</sub>) to carbon dioxide (CO<sub>2</sub>) versus

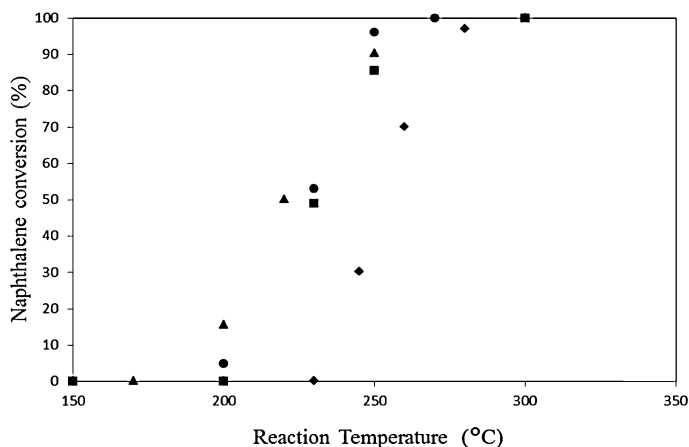


**Fig. 5** Catalytic activity in naphthalene combustion. Filled diamond CoO<sub>x</sub>(1)/SiO<sub>2</sub>, filled square CoO<sub>x</sub>(5)/SiO<sub>2</sub>, filled triangle CoO<sub>x</sub>(10)/SiO<sub>2</sub>, filled circle CoO<sub>x</sub>(15)/SiO<sub>2</sub>

temperature, using the O<sub>2</sub>/He mixture as oxidizing agent. All the supported cobalt catalysts decrease the combustion temperature of naphthalene (Table 3). The catalytic activity depends on the metal loading, the catalysts with higher loadings being the most active. As the cobalt content increases, the T50 of the reaction decreases and the T100 is reached at lower temperatures than the observed without catalyst. The CoO<sub>x</sub>(15)/SiO<sub>2</sub> catalyst, the most active one, reaches T100 at 270 °C, which is a very low combustion temperature.

According to EDS and TPR results, with increasing the nominal cobalt concentration, both the cobalt surface content and the reducibility of Co<sub>3</sub>O<sub>4</sub> supported species increase. TPR diagrams indicate that the reduction signals start at lower temperature and the area of these signals increase, especially for the reduction signal located in the low-interaction region, 250–450 °C. These reducible Co<sub>3</sub>O<sub>4</sub> species are proposed as active sites for naphthalene combustion. For bulk copper manganese oxide catalysts, Clarke et al. suggest a direct relationship between the activity for naphthalene combustion and the extent of catalysts reduction [24]. The authors suggest that the lability of oxygen species is important for naphthalene combustion reaction.

Silica supported cobalt catalysts show a different relationship between concentration and activity for the naphthalene combustion, as that observed for the propane combustion. While the CoO<sub>x</sub>(5)/SiO<sub>2</sub> is the most catalyst most for the propane combustion and an increase of the cobalt concentration causes a decrease of the activity, for the naphthalene combustion the catalyst with the highest loading is the most active.

These differences can be attributed to the different types of C–C bonds present in both molecules and also to their different molecular size which, in turn, can lead to the existence of several possible mechanisms. In this sense, other authors have reported that the performance of catalysts for saturated linear hydrocarbons is not similar to the observed for aromatic hydrocarbons [15, 25].

## Conclusion

Silica-supported catalysts showing very good activity in the combustion reaction of propane with 8 % oxygen, in the presence and in the absence of NO, were synthesized.  $\text{CoO}_x(5)/\text{SiO}_2$  is the most active catalyst for the combustion of propane. A good dispersion of supported oxide phases,  $\text{Co}_3\text{O}_4$ , was achieved with this catalyst. It is suggested that the catalytic activity may be correlated with the presence of cobalt oxide phases that are reducible at low temperature and have low interaction with the catalytic support.

The catalysts are also active in the combustion reaction of naphthalene and substantially decrease the combustion temperatures of this hydrocarbon.

**Acknowledgments** The authors acknowledge the financial support of CONICET, ANPCyT and UNLP; Eng. Edgardo Soto for BET experiments and Mrs. Mariela Theiller for SEM–EDS measurements.

## References

1. Pfefferle LD, Pfefferle WC (1987) *Catal Rev Sci Eng* 29:219–267
2. Choudhary TV, Banerjee S, Choudhary VR (2002) *Appl Catal A* 234:1–23
3. Gololobov AM, Bekk IE, Bragina GO, Zaikovskii VI, Ayupov AB, Telegina NS, Bukhtiyarov VI, Stakheev AY (2009) *Kinet Catal* 50:830–836
4. Kim KB, Kim YH, Song KS, Park ED (2011) *Rev Adv Mater Sci* 28:35–39
5. Garetto TF, Rincón E, Apesteguía CR (2007) *Appl Catal B* 73:65–72
6. Demoulin O, Le Clef B, Navez M, Ruiz P (2008) *Appl Catal A* 344:1–9
7. Yoshida H, Yazawa Y, Hattori T (2003) *Catal Today* 87:19–28
8. García T, Agouram S, Taylor SH, Morgan D, Dejoz A, Vázquez I, Solsona B (2015) *Catal Today* 254:12–20
9. Baldi M, Escribano VS, Amores JMG, Milella F, Busca G (1998) *Appl Catal B* 17:175–182
10. Skaf M, Aouad S, Hany S, Cousin R, Abi-Aad E, Aboukaïs A (2014) *J Catal* 320:137–146
11. Aboukaïs A, Abi-Aad E, Taouk B (2013) *Mater Chem Phys* 142:564–571
12. Sellick DR, Aranda A, García T, López JM, Solsona B, Mastral AM, Morgan DJ, Carley AF, Taylor SH (2013) *Appl Catal B* 132–133:98–106
13. García T, Sellick D, Varela F, Vázquez I, Dejoz A, Agouram S, Taylor SH, Solsona B (2013) *Appl Catal A* 450:169–177
14. Ntainjua E, Taylor SH (2009) *Top Catal* 52:528–554
15. García T, Solsona B, Taylor SH (2006) *Appl Catal B* 66:92–99
16. Jones A, McNicol B (1986) *Temperature programmed reduction for solid material characterization*. Marcel Dekker Inc, New York
17. Vetere V, Merlo AB, Ruggera JF, Casella ML (2010) *J Braz Chem Soc* 21:914–920
18. Girardon JS, Lermontov AS, Gengembre L, Chernavskii PA, Griboval-Constant A, Khodakov AY (2005) *J Catal* 230:339–352
19. Brik Y, Kacimi M, Ziyad M, Bozon-Verduraz F (2001) *J Catal* 202:118–128
20. Voß M, Borgmann D, Wedler G (2002) *J Catal* 212:10–21
21. Khodakov AY, Lynch J, Bazin D, Rebours B, Zanier N, Moisson B, Chaumette P (1997) *J Catal* 168:16–25
22. Storsæter S, Tøtdal B, Walmsley JC, Tanem BS, Holmen A (2005) *J Catal* 236:139–152
23. Mrad R, Cousin R, Poupin C, Aboukaïs A, Siffert S (2015) *Catal Today* 257:98–103
24. Clarke TJ, Kondrat SA, Taylor SH (2015) *Catal Today* 258:610–615
25. García T, Solsona B, Cazorla-Amoros D, Linares-Solano A, Taylor SH (2006) *Appl Catal B* 62:66–76